THE JOURNAL OF BIOLOGICAL CHEMISTRY VOL. 286, NO. 49, pp. 42446–42458, December 9, 2011

Alteration of Ceramide Synthase 6/C_{16}-Ceramide Induces Activating Transcription Factor 6-mediated Endoplasmic Reticulum (ER) Stress and Apoptosis via Perturbation of Cellular Ca^{2+} and ER/Golgi Membrane Network*[S]

Received for publication, July 28, 2011, and in revised form, October 18, 2011 Published, JBC Papers in Press, October 19, 2011, DOI 10.1074/jbc.M111.287383

Can E. Senkal[‡], Suriyan Ponnusamy[‡], Yefim Manevich[§], Marisa Meyers-Needham[‡], Sahar A. Saddoughi[‡], Archana Mukhopadyay[‡], Paul Dent[¶], Jacek Bielawski[‡], and Besim Ogretmen[‡1]

From the [‡]Department of Biochemistry and Molecular Biology, Hollings Cancer Center and [§]Department of Cell and Molecular Pharmacology and Experimental Therapeutics, Medical University of South Carolina, Charleston, South Carolina 29425 and the [¶]Department of Neurosurgery, Virginia Commonwealth University, Richmond, Virginia 23298

Background: Mechanisms of ATF-6 activation and apoptosis by CerS6/C_{16}-ceramide knockdown remain unknown.
Results: ATF-6 was activated by a concerted two-step process; that is, the release of Ca^{2+} from the ER, which disrupted ER/Golgi membranes via CerS6/C_{16}-ceramide alteration.
Conclusion: CerS6/C_{16}-ceramide controls ER Ca^{2+} homeostasis and the ER/Golgi membrane integrity, which regulates ATF-6.
Significance: These data will define distinct roles of CerS6/C_{16}-ceramide in apoptosis.

Mechanisms that regulate endoplasmic reticulum (ER) stress-induced apoptosis in cancer cells remain enigmatic. Recent data suggest that ceramide synthase1–6 (CerS1–6)-generated ceramides, containing different fatty acid chain lengths, might exhibit distinct and opposing functions, such as apoptosis *versus* survival in a context-dependent manner. Here, we investigated the mechanisms involved in the activation of one of the major ER stress response proteins, ATF-6, and subsequent apoptosis by alterations of CerS6/C_{16}-ceramide. Induction of wild type (WT), but not the catalytically inactive mutant CerS6, increased tumor growth in SCID mice, whereas siRNA-mediated knockdown of CerS6 induced ATF-6 activation and apoptosis in multiple human cancer cells. Down-regulation of CerS6/C_{16}-ceramide, and not its further metabolism to glucosylceramide or sphingomyelin, activated ATF-6 upon treatment with ER stress inducers tunicamycin or SAHA (suberoylanilide hydroxamic acid). Induction of WT-CerS6 expression, but not its mutant, or ectopic expression of the dominant-negative mutant form of ATF-6 protected cells from apoptosis in response to CerS6 knockdown and tunicamycin or SAHA treatment. Mechanistically, ATF-6 activation was regulated by a concerted two-step process involving the release of Ca^{2+} from the ER stores ($[Ca^{2+}]_{ER}$), which resulted in the fragmentation of Golgi membranes in response to CerS6/C_{16}-ceramide alteration. This resulted in the accumulation of pro-ATF-6 in the disrupted ER/Golgi membrane network, where pro-ATF6 is activated. Accordingly, ectopic expression of a Ca^{2+} chelator calbindin prevented the Golgi fragmentation, ATF-6 activation, and apoptosis in response to CerS6/C_{16}-ceramide down-regulation. Overall, these data suggest a novel mechanism of how CerS6/C_{16}-ceramide alteration activates ATF6 and induces ER-stress-mediated apoptosis in squamous cell carcinomas.

A significant number of ER[2] resident proteins either sequester Ca^{2+} or function as molecular chaperones to monitor proper protein folding. Failure to fold newly synthesized ER client proteins or perturbation of $[Ca^{2+}]_{ER}$ results in ER stress (1, 2). A complex homeostatic mechanism, unfolded protein response, minimizes ER stress (1, 2). The unfolded protein response is mediated through three ER transmembrane proteins: inositol-requiring enzyme 1 (IRE-1), pancreatic ER kinase (PKR)-like ER kinase (PERK), and activating transcription factor 6 (ATF6), which have distinct targets and functions (3–5). After dissociation from GRP78 (2, 6), ATF6 translocates to the Golgi, where it is cleaved into its active form by site-1 or site-2 proteases (S1P and S2P) (7, 8). Active ATF6 then moves to the nucleus and induces genes with an ER stress response element in their promoter. The identified targets of ATF6 include GRP78, GRP94, protein disulfide isomerase, XBP1, and CHOP (growth arrest and DNA damage-inducible gene 153 (GADD153)) (9–11). Induction of CHOP down-regulates Bcl2 and mediates apoptosis (12, 13). However, upstream mechanisms, which selectively activate ATF-6 but not IRE-1 or pan-

* This work was supported, in whole or in part, by National Institutes of Health Grants CA088932, DE016572, and CA097132.
[S] The on-line version of this article (available at http://www.jbc.org) contains supplemental Figs. 1–3.
[1] To whom correspondence should be addressed: 86 Jonathan Lucas St., HO512, Charleston, SC 29425. Tel.: 843-792-0940; Fax: 843-792-2556; E-mail: ogretmen@musc.edu.

[2] The abbreviations used are: ER, endoplasmic reticulum; IRE-1, inositol-requiring enzyme 1; ATF6, activating transcription factor 6; S1P and S2P, site-1 and site-2 proteases, respectively; CERT, ceramide transport protein; SM, sphingomyelin; GlcCer, glucosylceramide; Q-PCR, quantitative real-time PCR; Tet, tetracycline; TRITC, tetramethylrhodamine isothiocyanate; NLS, nuclear localization signal; BFA, brefeldin A; Scr, scrambled; SMS1 or SMS2, SM synthase 1 or 2, respectively; SERCA, sarco(endo)plasmic reticulum calcium ATPase; Q-PCR, quantitative real-time PCR; ThG, thapsigargin; Endo H, endoglycosidase H; GM3, NeuAcα2,3Galβ1,4Glc-ceramide; SAHA, suberoylanilide hydroxamic acid; GM1, Galβ1,3GalNAcβ1,4(NeuAcα2,3)-Galβ1,4Glc-ceramide; GM2, GalNAcβ4[NeuAcα3]Galβ4Glcβ1-ceramide.

creatic ER kinase (PKR)-like ER kinase, leading to CHOP-induced apoptosis in cancer cells, are unknown.

De novo ceramide synthesis by CerS1–6 takes place in the ER, and ceramide is transported to the Golgi by ceramide transport protein (CERT) or FABB2 for the generation of sphingomyelin (SM) or glucosylceramide (GlcCer), respectively (14, 15). CerS exerts a preference for the generation of endogenous ceramides with distinct fatty acid chain lengths (16–18). For example, the CerS1/Cer4 mainly generate C_{18}-ceramide (19), whereas CerS5–6 preferentially mediates the generation of C_{16}-ceramide (20).

Our unexpected and novel previous data showed that overexpression of CerS6 and increased C_{16}-ceramide play pro-survival roles, and down-regulation of CerS6 induces apoptosis through specific activation of the ATF6-CHOP arm of the unfolded protein response pathway in HNSCC cell lines (21). However, mechanisms by which knockdown of CerS6/C_{16}-ceramide induces ATF-6 activation and subsequent apoptosis remain unknown. In this study we defined a novel mechanism that regulates ATF-6-dependent apoptosis via a concerted two-step process involving perturbation of the $[Ca^{2+}]_{ER}/[Ca^{2+}]_{In}$ rheostat and ER/Golgi membrane network in response to down-regulation of CerS6/C_{16}-ceramide generation.

EXPERIMENTAL PROCEDURES

Cell Lines and Culture Conditions—HNSCC cell lines were cultured as described previously (21). Lung cancer cell lines A549, H157, and H1650 were cultured in DMEM with 10% FBS and 1% penicillin and streptomycin.

Transfections and siRNAs—Non-targeting (Scramble) and CerS6 siRNAs used were as described (21). All other siRNAs (siGenome SMARTpool) used in the study were obtained from Dharmacon. Plasmid and siRNA transfections were carried out using Effectene (Qiagen) and Oligofectamine (Invitrogen) transfection reagents, respectively.

Q-PCR and Western Blotting—Quantitative real-time PCR with TaqMan gene expression kits (Applied Biosystems) and Western blotting were carried out as described previously (21). Antibodies used in the study are as follows: anti-CerS6 (Abnova), anti-actin and (Sigma), anti-calnexin and anti-calreticulin (Santa Cruz Biotechnology), anti-V5 (Invitrogen), anti-SERCA2 and anti-SERCA3 (Cell Signaling Technology), anti-CERT (Bethyl Laboratories), and anti-I2PP2A (Globozyme).

Measurement of Ceramides—Ceramides were measured by LC/MS/MS and normalized to total inorganic phosphate (P_i) as described (22).

Caspase-3 Activity Assay—Caspase-3 activity was measured by fluorometry using caspase-3 activity assay kit (R&D Systems) as described by the manufacturer.

Measurement of HNSCC Tumor Growth in SCID Mice—HNSCC cell xenografts were generated by injecting UM-SCC-22A cells stably expressing tetracycline (Tet)-inducible wild type or catalytically inactive mutant (H212A) CerS6 in the flanks of SCID mice. After the tumors were grown to at least 25 mm^3, Tet (1 mg/ml) was included in the drinking water of the mice to turn on the gene expression. Tumor size was measured every 4 days and calculated as described (23). Data obtained from measurements were analyzed using Tukey's Student range test, as described (23). All the procedures related to mice were approved by the Institutional Animal Care and Use Committee at Medical University of South Carolina.

Fluorescent Detection of Intracellular Ca^{2+}—Cells were grown on Aclar plastic slides (Electron Microscopy Sciences, Hatfield, PA) to ~90% confluence and were incubated with 5 μM Fluo-3-AM (Invitrogen) for 45 min in complete media at 37 °C. Labeled cells were washed 3 times with PBS containing 100 μM $CaCl_2$ or 4 mM EGTA and used for $[Ca^{2+}]_{In}$ detection. Fluorescent measurement of intracellular Ca^{2+} was performed with the use of a PTI QM-4 (PTI Inc., Birmingham, NJ) spectrofluorometer and time-based (resolution 0.1 s) fluorescence detection using standard Felix-32 (PTI) software. The slide with adhered labeled cells was placed in 10 × 10 × 40-mm quartz cuvette with PBS (on diagonal at 45° to an excitation (490 nm) beam) under permanent stirring at 37 °C. Emission of Fluo-3-Ca^{2+} complex (526 nm) was recorded for 100 s (24). All measurements were corrected for the fluorescence of unlabeled cells adhered to the slide, and DMSO was used as a vehicle control. All experiments were done in triplicate, and results represent the mean ± S.D.

Immunofluorescence and Confocal Microscopy—For $[Ca^{2+}]_{In}$ visualization, cells were grown on glass coverslips in 6-well plates. After the siRNA transfections, cells were treated with 5 μM Fluo-4-AM (Invitrogen) for 45 min in complete media at 37 °C. Immunofluorescent staining of GM130, calnexin, and FLAG-ATF-6 was carried out as described (25). Briefly, cells were washed with PBS and fixed in 4% paraformaldehyde at 25 °C for 10 min. After permeabilization with 0.1% Triton X-100 in PBS, the cells were blocked in 1% BSA for 1 h. Cells were incubated with primary antibodies against GM130, calnexin (Santa Cruz Biotechnology), and anti-FLAG (M2, Sigma) in 1% BSA for 1 h. Then cells were incubated with secondary antibodies conjugated with FITC or TRITC (Jackson ImmunoResearch). The images were visualized using Leica TCS SP2 AOBS laser scanning confocal microscope in the presence of Pro-Long Gold antifade reagent (Invitrogen).

Measurement of Anchorage-independent Growth—Anchorage-independent growth was measured as growth of cells on soft agar as described (26).

Generation of ER-targeted I2PP2A and Determination of Carbohydrate Chain Modification of I2PP2A-ER via Fusion of the Golgi with the ER Membranes—The expression vector containing the ER-targeted I2PP2A with the green fluorescent protein (GFP) (I2PP2A-ER-GFP) was constructed by first sequential deletion of nuclear localization signals (NLS1 and NLS2) and then by the addition of KDEL, the ER retention signal at the C terminus using site-directed mutagenesis with the following primers: NLS1 forward (5′-GATCTCGAGATGTCGAACTCCAACCACGAC-3′, NLS1 reverse; 5′-GTCGTGGTTGGAGTTCGACATCTCCAGATC-3′; NLS2 forward (5′-TCTGGAAAGGATTTGACGCAGCATGAGGAACC-3′, NLS2 reverse; 5′-GGTTCCTCATGCTGCGTCAAATCCTTTCCAGA-3′); ER retention forward (5′-GATGAAGGAGAAGATGACAAAGATGAACTCTAGGAATTTTGCAGTCGACGGTACCG-3′), ER retention reverse (5′-CGGTACCGTCGACTGCAGAATTCCTAGAGTTCATCTTTGTCATCTTCTCCTTCATC-3′). Carbohydrate modification status of

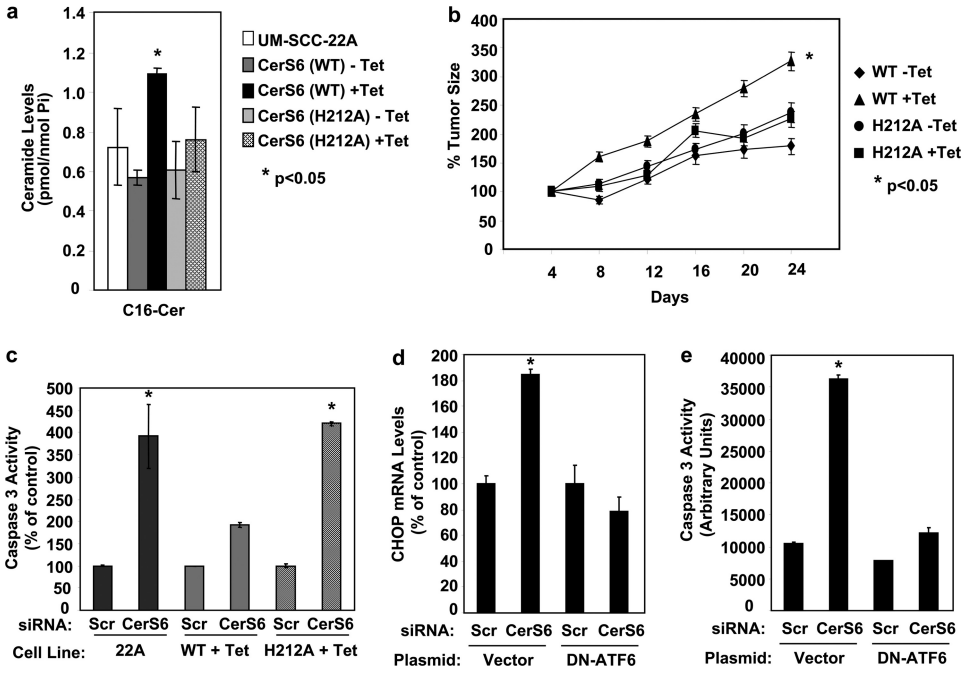

FIGURE 1. **Down-regulation of CerS6 activates ATF-6/CHOP arm or unfolded protein response leading to caspase-3 activation.** *a*, C_{16}-ceramide levels were measured by LC/MS in Tet in UM-SCC-22A cells untransfected or stably transfected with Tet-inducible WT or catalytically inactive mutant (H212A) CerS6 with or without Tet. *b*, xenografts of UM-SCC-22A cells expressing WT or mutant (H212A) CerS6 under Tet-inducible promoter were generated on SCID mice, and their growth was measured by calipers every 4 days ($n = 6$ for each group). *c*, control UM-SCC-22A (*22A*) cells and Tet-induced (+*Tet*) UM-SCC-22A cells expressing either WT or H212A mutant of CerS6 under Tet-inducible promoter were transfected with either non-targeting (Scr) or CerS6 siRNA (50 nM, 48 h), and caspase 3 activity was measured as described under "Experimental Procedures." *d* and *e*, UM-SCC-22A cells were transiently transfected with control (*Vector*) or dominant-negative ATF-6 (*DN-ATF6*)-expressing plasmids. After 48 h the cells were transfected with Scr or CerS6 siRNAs (50 nM, 48 h), and CHOP mRNA expression and caspase 3 activity were measured by quantitative real-time PCR (Q-PCR) and a caspase 3 activity assay kit, respectively. In *a*, *c*, *d*, and *e* graphs show the mean ± S.E. from three independent experiments performed in duplicates. Student's *t* test was performed and $p < 0.05$ (*) was considered significant.

I2PP2A-ER-GFP was evaluated by Endo H cleavage *in vitro*. In summary, cells expressing I2PP2A-ER-GFP or I2PP2A-WT-GFP were treated with brefeldin A (BFA) and CerS6 or scrambled (Scr) siRNAs. Cell lysates (15–30 μg of total protein) were then treated with Endo H (New England Biolabs) at 37 °C for 2 h. I2PP2A-ER-GFP and nuclear I2PP2A-WT-GFP or endogenous I2PP2A was detected by SDS-PAGE and Western blotting using the anti-I2PP2A antibody.

Statistical Analysis—Student's *t* test was used to analyze the data, and $p < 0.05$ was considered significant.

RESULTS

Induction of CerS6 Expression and C_{16}-ceramide Generation Results in Increased Tumor Growth in SCID Mice—Our previous studies unexpectedly showed that knockdown of CerS6 resulted in apoptosis, suggesting a pro-survival role (21), consistent with increased CerS6/C_{16}-ceramide in the majority of primary HNSCC tumors compared with adjacent non-cancerous head and neck tissues (27). To investigate the possible pro-survival role of CerS6-generated C_{16}-ceramide, we first examined the growth of UM-SCC-22A cell-derived xenografts in SCID mice, which were stably transfected with tetracycline-inducible lentiviral expression vectors containing WT or the catalytically inactive H212A mutant of CerS6, which does not generate C_{16}-ceramide. The data show that induction of WT-CerS6 expression, but not its catalytically inactive mutant, increased C_{16}-ceramide generation about 1.5-fold compared with controls (Fig. 1*a*). Importantly, CerS6/C_{16}-ceramide induction significantly enhanced HNSCC tumor growth (about 2-fold, $p < 0.05$) compared with controls, whereas expression of the mutant CerS6 did not have any significant effect on tumor growth *in vivo* (Fig. 1*b*). These data suggest a role for Cer6/C_{16}-ceramide in enhancing HNSCC tumor growth, contrary to the general tumor suppressive roles of C_{16}-ceramide.

Down-regulation of CerS6 Mediates Apoptosis via ATF-6 Activation—Because induction of CerS6/C_{16}-ceramide induced HNSCC tumor growth, we next determined whether down-regulation of CerS6 mediates apoptosis. Knockdown of CerS6 using siRNAs increased caspase-3 activity, which was prevented by the induction of WT, but not the catalytically inactive mutant of CerS6, compared with Scr non-targeting siRNA-transfected controls in UM-SCC-22A cells (Fig. 1*c*). Consistent with previous data (21), down-regulation of CerS6 increased ATF-6 activation, as determined by increased expression of its down-stream target CHOP expression (Fig. 1*d*). More importantly, ectopic expression of the dominant-negative mutant (28) of ATF-6 completely prevented CHOP expression and caspase activation in response to knockdown of CerS6 (Fig. 1, *d* and *e*, respectively). Also, knockdown of CerS6 using siRNA induced apoptosis via ATF6/CHOP activation in UM-SCC-1 and UM-SCC-14A cells (Fig. 2*a*). Importantly, activation of CHOP in response to CerS6 knockdown was dependent on the activation of ATF-6, but not IRE-1 or ATF-4, because down-regulation of endogenous ATF-6, but not IRE-1 or ATF-4, protected caspase-3 activation in response to CerS6 knockdown (Fig. 2*b*). Interestingly, CerS6 knockdown also activated CHOP in H1650 human squamous lung cancer cells (Fig.

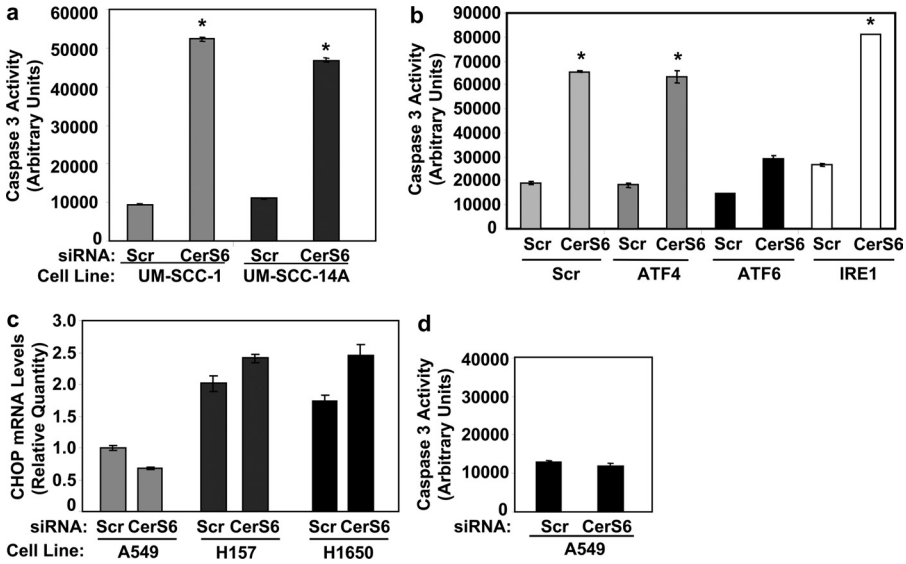

FIGURE 2. **Effects of down-regulation of CerS6/C_{16}-ceramide in HNSCC and lung cancer cell lines.** *a*, UM-SCC-1 and UM-SCC-14A cells were transfected with either Scr or CerS6 siRNA (50 nM, 48 h), and activation of caspase 3 was measured by caspase 3 activity assay kit. *b*, UM-SCC-22A cells were transfected with either of Scr, ATF4, ATF6, or IRE-1 siRNAs (50 nM, 48 h) before transfections with either Scr or CerS6 siRNAs (50 nM, 48 h), and their roles on caspase 3 activation were detected. *c* and *d*, A549, H157, and H1650 cells were transfected with either Scr or CerS6 siRNAs (50 nM, 48 h), and CHOP mRNA (*c*) and caspase 3 activation (*d*) was determined by Q-PCR and caspase 3 activity assay kit, respectively. Graphs show the mean ± S.E. from three independent experiments performed in duplicate. Student's *t* test was performed, and $p < 0.05$ (*) was considered significant.

2*c*), but it did not have any significant effect on CHOP expression and caspase-3 activation in human lung adenocarcinoma cell lines H157 or A549 cells (Fig. 2, *c* and *d*, respectively). These data suggest that knockdown of CerS6 induces caspase-mediated apoptosis via selective activation of the ATF-6/CHOP axis in various human cancer cell lines with a squamous carcinoma origin.

A Known ER Stress Inducer Tunicamycin Mediates CerS6 Degradation and Subsequent ATF-6 and Caspase-3 Activation—We then examined whether down-regulation of CerS6 can be mediated by a known ER stress inducer, tunicamycin, without using siRNAs, which then results in ATF-6 activation. Treatment with tunicamycin at 0.05–0.5 μg/ml decreased the expression of CerS6 protein but not other ER resident proteins calreticulin or calnexin (Fig. 3*a*) without decreasing CerS6 mRNA (supplemental Fig. 1). Tunicamycin did not seem to alter the glycosylation of CerS6 protein because treatment with peptide *N*-glycosidase, which removes glycosyl residues from proteins, did not show any differences in the decreased glycosylated CerS6 in response to tunicamycin (Fig. 3*b*). Tunicamycin-induced decrease in CerS6 protein was partially rescued by an inhibitor of proteasome (MG-132) but not by cathepsin B or cathepsin D inhibitors (Ca074 and pepstatin A, respectively), suggesting the involvement of proteasomal degradation (Fig. 3*c*). Accordingly, induction of WT-Cer6 expression using Tet (confirmed by Western blotting using anti-CerS6 antibody as shown in Fig. 3*d*) prevented activation of ATF-6, as measured by CHOP expression, and down-regulation of Bcl-2 compared with uninduced controls (Fig. 3*e*, *right* and *left panels*, respectively). Moreover, treatment with tunicamycin significantly inhibited the growth of UM-SCC-22A cells on soft agar (about 60 or 50%, $p < 0.05$) compared with untransfected or un-induced controls, respectively (Fig. 3*f*). Importantly, induction of wt-CerS6 expression slightly but significantly prevented growth inhibitory effects of tunicamycin in these cells (Fig. 3*f*). Thus, these data suggest that induction of proteasomal degradation of CerS6 by tunicamycin treatment results in activation of ATF-6 and subsequent apoptosis.

Similar data were also obtained when cells were treated with an histone deacetylase inhibitor SAHA, which induces ER stress-mediated apoptosis (29). Treatment with SAHA resulted in the degradation of endogenous CerS6 protein, activation of ATF-6/CHOP and caspase-3 (Fig. 4, *a–c*, respectively). Knockdown of ATF-6 using siRNAs protected the activation of ATF-6 and CHOP in response to SAHA (Fig. 4*d*). Moreover, induction of wt-CerS6 expression, but not its catalytically inactive mutant, partially but statistically significantly (about 50%, $p < 0.05$) protected caspase-3 activation in response to SAHA (Fig. 4*e*). Collectively, these data suggest that pharmacologic treatment with tunicamycin or SAHA, which are known to induce ER stress, results in down-regulation of CerS6 and induces ATF-6 activation, similar to the effects of siRNA-mediated knockdown of CerS6.

Activation of ATF-6 by Knockdown of CerS6 Is Dependent on the Down-regulation of C16-ceramide but Not on Inhibition of Its Further Metabolism to C16-GlcCer or C16-SM—To determine whether down-regulation of CerS6 induces ATF-6/CHOP activation and apoptosis due to decreased C_{16}-ceramide, C_{16}-GlcCer, and/or C_{16}-SM generation, we first down-regulated CerS6, glucosylceramide synthase (supplemental Fig. 2*a*), and SM synthases 1 or 2 (SMS1 or SMS2) using siRNAs and then determined their selective effects on CHOP expression. As expected, knockdown of CerS6 activated CHOP about 2-fold compared with controls, whereas down-regulation of glucosylceramide synthase did not have any significant effect on CHOP expression (Fig. 5*a*). Then, to determine whether reconstitution of C_{16}-ceramide generation rescues ATF-6/CHOP activation, we determined the effects of overexpression of WT *versus*

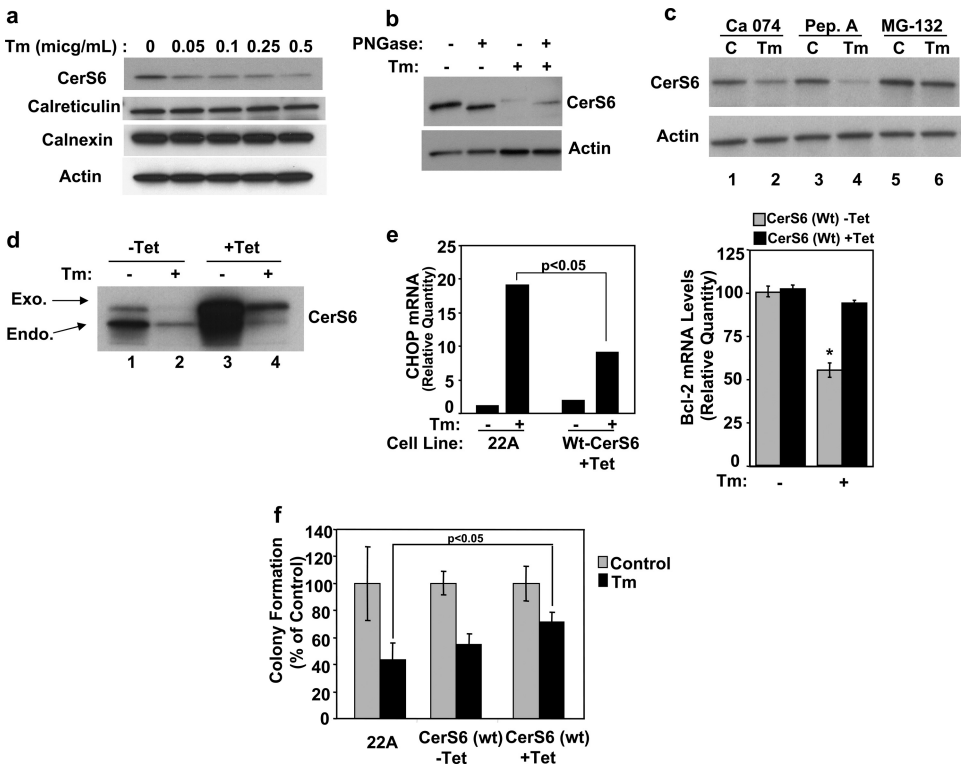

FIGURE 3. **Tunicamycin-induced ATF-6 activation is partially mediated by proteasomal degradation of CerS6.** *a*, UM-SCC-22A cells treated with various concentrations (0.05–0.5 μg/ml) tunicamycin (*Tm*) for 8 h, and protein levels of CerS6, calreticulin, calnexin, and actin were detected by Western blotting. *micg*, μg. *b*, protein extracts from UM-SCC-22A cells untreated or treated with tunicamycin (0.1 μg/ml, 8 h) were treated with peptide *N*-glycosidase (*PNGase*) as described under "Experimental Procedures," and CerS6 protein expression and molecular weight shift were detected by Western blotting. *c*, UM-SCC-22A cells were pretreated with Ca074, pepstatin A (*Pep. A*), or MG-132 for 1 h before treatment with tunicamycin (0.1 μg/ml, 8 h), and CerS6 and actin were detected by Western blotting. *C*, control. *d*, uninduced or Tet-induced cells expressing wild type CerS6 were treated with Tm (0.1 μg/ml, 8 h), and exogenously expressed (*Exo*) or endogenous (*Endo*) CerS6 protein levels were detected by Western blotting. *e*, control UM-SCC-22A cells (*22A*) or Tet-inducible wild type CerS6 expressing cells with or without Tet induction were treated with Tm (0.1 μg/ml, 8 h), and CHOP (*left panel*) and Bcl-2 (*right panel*) mRNA levels were measured by Q-PCR. *f*, control UM-SCC-22A cells (*22A*) or Tet-inducible wild type CerS6-expressing cells were used to measure anchorage independent growth on soft agar with or without tunicamycin treatment as described under "Experimental Procedures." In *a–d*, blots represent three independent experiments. In *e* and *f*, graphs show the mean ± S.E. from three independent experiments performed in duplicate. Student's *t* test was performed, and $p < 0.05$ (*) was considered significant.

the mutant CerS6 induction on CHOP expression in response to knockdown of CerS6. Data show that Tet induction of WT-CerS6, but not its mutant, prevented CHOP activation in response to CerS6 knockdown (Fig. 5*a*). We then examined whether conversion of C_{16}-ceramide to C_{16}-GlcCer plays a role in the protection effects of WT-CerS6 induction on ATF-6/CHOP activation in response to CerS6 knockdown. We hypothesized that if the conversion of C_{16}-ceramide to C_{16}-GlcCer is required for the protection of CHOP activation, then knockdown of glucosylceramide synthase should prevent the protective effects of wt-CerS6 induction on CHOP expression when endogenous CerS6 is down-regulated. Our present data show that down-regulation of glucosylceramide synthase did not significantly prevent the rescue of CHOP activation by WT-CerS6 induction in response to CerS6 knockdown (Fig. 5*a*). Down-regulation of GM3 synthase using siRNA also did not have any significant effect on ATF-6 activation in the absence/presence of WT-CerS6 induction in response to CerS6 siRNA (supplemental Fig. 2*b*). Thus, these data suggest that down-regulation of C_{16}-ceramide, but not C_{16}-GlcCer, or gangliosides induce ATF-6 activation and subsequent cell death in response to CerS6 knockdown.

To examine whether alteration of C_{16}-ceramide conversion to C_{16}-SM plays a role in the regulation of ATF-6/CHOP activation, we studied the effects of down-regulation of SMS1 or SMS2 on the protective effects of wt-CerS6 on CHOP expression in response to knockdown of endogenous CerS6. Interestingly, although knockdown of SMS2, but not SMS1, increased CHOP expression (Fig. 5*b*), SMS2 siRNA did not prevent the protective effects of wt-CerS6/C_{16}-ceramide on CHOP activation in response to CerS6 knockdown (Fig. 5*c*). It should be noted that down-regulation of SMS2 itself induced CHOP activation (Fig. 5, *b* and *c*), consistent with previously published effects on the induction of general ER stress (30, 31). Knockdown of both ATF6 and ATF4 using siRNAs protected CHOP activation in response to SMS2 siRNA (supplemental Fig. 2*c*), which is distinct from the effects of down-regulation of CerS6/C_{16}-ceramide on selective activation of ATF-6 but not ATF-4 or IRE-1. In addition, we also tested the effects of prevention of SM generation via down-regulation of CERT (14) on CHOP and REDD1, which are downstream targets of ATF-6 and ATF-4, respectively. Interestingly, we did not observe any increase in CHOP or REDD1 expression upon down-regulation of CERT (supplemental Fig. 2*d*), indicating that down-regulation of C_{16}-ceramide, but not C_{16}-SM generation, induces ATF-6 activation when CerS6 is down-regulated. Overall, these data suggest that down-regulation of C_{16}-ceramide, but not C_{16}-GlcCer/

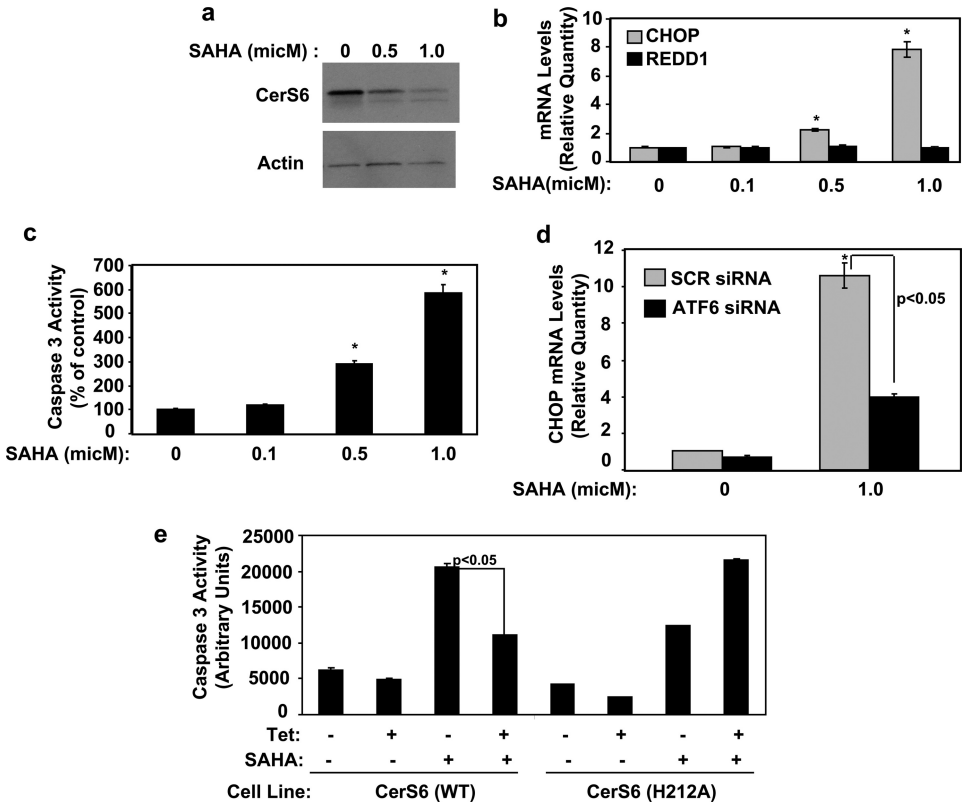

FIGURE 4. **Down-regulation of CerS6/C_{16}-ceramide by SAHA partially mediates activation of ATF-6/CHOP/caspase 3 axis of ER stress pathway.** *a*, UM-SCC-22A cells were treated with the indicated amounts of SAHA for 48 h and, CerS6 and actin protein levels were detected by Western blotting. *micM*, μM. *b* and *c*, cells were treated with SAHA for 48 h, and mRNA expression of CHOP and REDD1 (*b*) and activation of caspase 3 (*c*) were determined by Q-PCR and the caspase 3 activity assay kit, respectively. *d*, effects of ATF-6 down-regulation by siRNA (50 nM, 48 h) on SAHA (1 μM, 48 h) induced CHOP mRNA expression was determined by Q-PCR. *e*, cells stably expressing Tet-inducible wild type or catalytically inactive mutant (H212A) CerS6 was uninduced (−*Tet*) or induced (+*Tet*) and treated with SAHA (1 μM, 48 h), and their effects on caspase 3 activity were measured by caspase 3 activity assay kit. In *a*, blot pictures are representative of two independent experiments. Graphs show the mean ± S.E. from three independent experiments performed in duplicate. Student's *t* test was performed, and $p < 0.05$ (*) was considered significant.

GM3 or C_{16}-SM, plays a role in the activation of ATF-6/CHOP axis in response to CerS6 knockdown.

Down-regulation of CerS6/C_{16}-ceramide Results in Enhanced Ca^{2+} Release from ER Stores, Which Is Necessary for ATF-6 Activation—It is well established that the ER regulates Ca^{2+} homeostasis, and perturbation of $[Ca^{2+}]_{ER}$ signaling with increasing intracellular Ca^{2+} ($[Ca^{2+}]_{In}$) activates ATF-6 (28). Thus, we examined the effects of siRNA-mediated CerS6 knockdown on $[Ca^{2+}]_{In}$ using fluorescent (Fluo3-AM, Fluo4-AM) labeling and a real-time emission kinetics detection or confocal imaging. Remarkably, knockdown of CerS6 using siRNAs significantly increased $[Ca^{2+}]_{In}$ (about 6-fold, $p < 0.05$) compared with Scr siRNA-transfected controls (Fig. 6*a*, *left panel*). Similar data were also obtained when $[Ca^{2+}]_{In}$ elevation was detected by confocal microscopy using Fluo4-AM (Fig. 6*a*, *right panel*). Moreover, induction of WT-CerS6 with Tet completely prevented $[Ca^{2+}]_{In}$ elevation in response to CerS6 knockdown compared with uninduced controls (Fig. 6*b*). Thus, these data suggest that down-regulation of CerS6 results in elevation of $[Ca^{2+}]_{In}$, and reconstitution of C_{16}-ceramide generation by induction of WT-CerS6, but not with its catalytically inactive mutant, rescues this effect of CerS6 knockdown on increased $[Ca^{2+}]_{In}$.

Then, to determine whether increased $[Ca^{2+}]_{In}$ plays any roles in the regulation of ATF-6 activation and apoptosis in response to CerS6 knockdown, we used molecular Ca^{2+} chelator, calbindin D21 expression, and examined its effects on ATF-6 activity and apoptosis. First we confirmed the Ca^{2+} chelating effect of ectopic calbindin expression by measuring $[Ca^{2+}]_{In}$ using Fluo3. Calbindin expression reduced $[Ca^{2+}]_{In}$ levels about 50% (Fig. 6*c*). More importantly, Ca^{2+} chelating with expression of calbindin prevented the effects of CerS6 knockdown on ATF-6 activation and apoptosis, measured by increased CHOP expression and caspase-3 activity, respectively (Fig. 6, *d* and *e*, respectively). Thus, these data suggest that elevation of $[Ca^{2+}]_{In}$ in response to down-regulation of CerS6/C_{16}-ceramide plays key roles in ATF-6 activation and apoptosis.

To determine the source of elevated $[Ca^{2+}]_{In}$, we examined the effects of CerS6 knockdown on thapsigargin (ThG)-induced Ca^{2+} release from the ER/SR. The data showed that although ThG treatment resulted in the release of Ca^{2+} from the ER/SR, elevating $[Ca^{2+}]_{In}$ around 2-fold in Scr-siRNA-transfected controls, ThG did not have any significant effect on $[Ca^{2+}]_{In}$ in response to CerS6 knockdown (Fig. 7*a*). In addition to ThG, we examined the effects of CerS6 down-regulation on inositol 1,4,5-triphosphate-regulated Ca^{2+} response from ER stores. Treatment of Scr siRNA-transfected cells with 1-oleoyl-2-acyl-*syn*-glycerol, a known stimulator of Ca^{2+} release from ER stores via inositol 1,4,5-triphosphate receptors

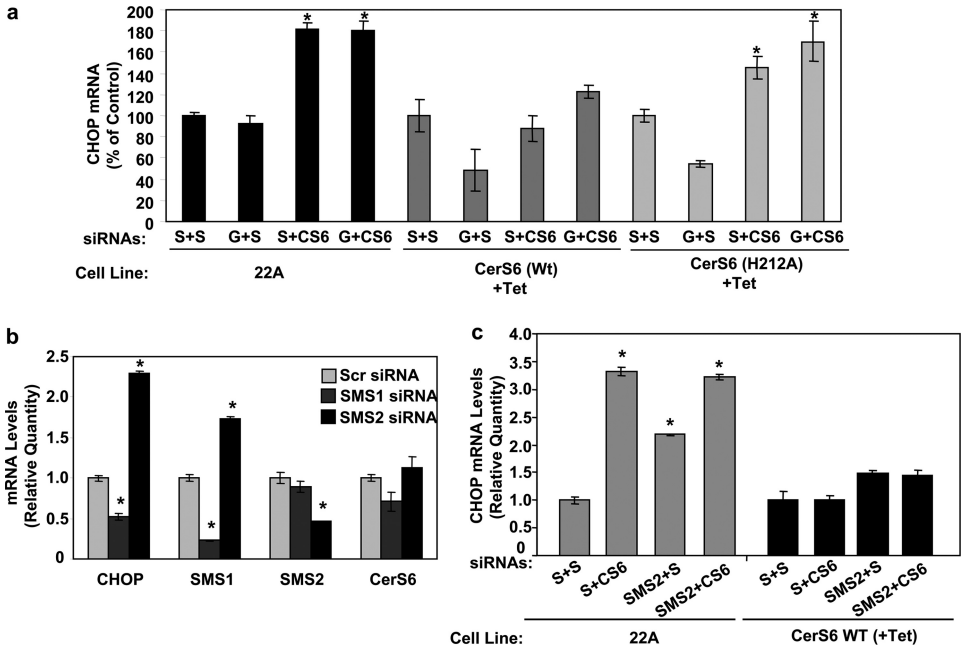

FIGURE 5. **Dissecting the roles of C_{16}-GlcCer and C_{16}-SM in the activation of ATF-6/CHOP arm of ER stress.** *a*, control UM-SCC-22A (*22A*) cells and Tet-induced (+*Tet*) UM-SCC-22A cells expressing either the WT or catalytically inactive mutant (*H212A*) CerS6 were transfected with Scr (*S*), glucosylceramide synthase (*G*), or CerS6 (*CS6*) siRNAs (50 nM) alone or in combination (*S*+*S*, *G*+*S*, *S*+*CS6*, and *G*+*CS6*) for 48 h, and CHOP mRNA levels were measured by Q-PCR. *b*, UM-SCC-22A cells were transfected with either Scr, SMS1, or SMS2 siRNAs (20 nM, 48 h), and CHOP, SMS1, SMS2, and CerS6 mRNA expression levels were measured by Q-PCR. *c*, control UM-SCC-22A (22A) cells and Tet-induced (+*Tet*) UM-SCC-22A cells expressing WT CerS6 were transfected with Scr (*S*), SMS2, or CerS6 (*CS6*) siRNAs (20 nM, 48 h) alone or in combination (*S*+*S*, *S*+*CS6*, *SMS2*+*S*, and *SMS2*+*CS6*), and CHOP mRNA expression was determined by Q-PCR. In *a*–*c* graphs show the mean ± S.E. from three independent experiments performed in duplicate. Student's *t* test was performed, and $p < 0.05$ (*) was considered significant.

(32), caused about a 6-fold increase in $[Ca^{2+}]_{In}$. In contrast, siRNA-mediated knockdown of CerS6 almost completely prevented 1-oleoyl-2-acyl-*syn*-glycerol-mediated $[Ca^{2+}]_{In}$ elevation in UM-SCC-22A cells (Fig. 7*b*). These data indicate that knockdown of CerS6 results in increased $[Ca^{2+}]_{In}$ possibly via depleting the $[Ca^{2+}]_{ER}$ stores.

To determine the mechanisms of $[Ca^{2+}]_{In}$ elevation, we examined the effects of CerS6 knockdown on the expression of SERCA2 and SERCA3, which regulate ER/cytoplasmic Ca^{2+} (33). Our data show that siRNA-mediated CerS6 knockdown decreased SERCA2 and SERCA3 mRNA and protein about 40% and compared with controls (Fig. 8, *a* and *b*, respectively). Moreover, induction of WT-CerS6 expression using Tet prevented the down-regulation of SERCA2 and SERCA3 in response to siRNA-mediated knockdown of CerS6 (Fig. 8, *c* and *d*, respectively). Interestingly, inhibition of ATF-6 by siRNA-mediated knockdown did not completely prevent $[Ca^{2+}]_{In}$ elevation or down-regulation of SERCA3 in response to CerS6 knockdown (Fig. 8, *e* and *f*, respectively). The chelating of calcium by calbindin expression prevented ATF-6 activation; however, inhibition of ATF6 expression did not have any effect on $[Ca^{2+}]_{In}$ or SERCA expression. It is suggested that perturbation of $[Ca^{2+}]_{In}$ by down-regulation of SERCA2/3 is an upstream regulator of ATF-6 activation and apoptosis in response to CerS6 knockdown. Overall, these data suggest that knockdown of CerS6 mediates the down-regulation of SERCA2/3, which in turn results in increased $[Ca^{2+}]_{In}$, leading to ATF-6 activation and apoptosis. It should be noted here that down-regulation of CerS6 did not have any detectable effect on IP-dependent Ca^{2+} pumps (34, 35), and pharmacological inhibition of these pumps did not prevent CHOP activation in response to CerS6-knockdown (supplemental Fig. 3).

Knockdown of CerS6 Results in $[Ca^{2+}]_{ER}$-dependent Golgi Membrane Fragmentation, Which Activates ATF-6—To determine whether down-regulation of SERCA2 and/or SERCA3 is sufficient to activate ATF-6 and apoptosis, we examined the effects of siRNA-mediated knockdown of SERCA2/3 on CHOP expression and caspase-3 activity. Interestingly, selective knockdown of SERCA2 and SERCA3 by about 80% compared with controls (measured by Q-PCR, Fig. 9*a*) did not cause any increase in CHOP mRNA or caspase-3 activation (Fig. 9, *b*–*d*), respectively). These data suggested that in addition to an increase in $[Ca^{2+}]_{In}$ via down-regulation of SERCA2/3, knockdown of CerS6 might have an additional effect, which is required for ATF-6 activation. It is known that pro-ATF-6 is cleaved sequentially by the Golgi resident proteases S1P and S2P, and then activated ATF-6 shuttles to the nucleus for transactivation of CHOP (8). Therefore, we determined whether CerS6 knockdown had any effects on the ER/Golgi membrane network using confocal microscopy after staining the cells with the anti-calnexin (*red*) and anti-GM130 (*green*) for visualization of ER and Golgi, respectively. The data showed that knockdown of CerS6 resulted in the fragmentation of Golgi, as noted by increased punctate-like formations of GM130 (*green punctate*), which also showed enhanced co-localization of GM130 with calnexin (*yellow*) compared with control cells (Fig. 9*e*). Increased co-localization of ER and Golgi markers calnexin and GM130 suggested that knockdown of CerS6 resulted in increased Golgi membrane fragmentation, some of which co-localized with the ER membranes, which in turn might have

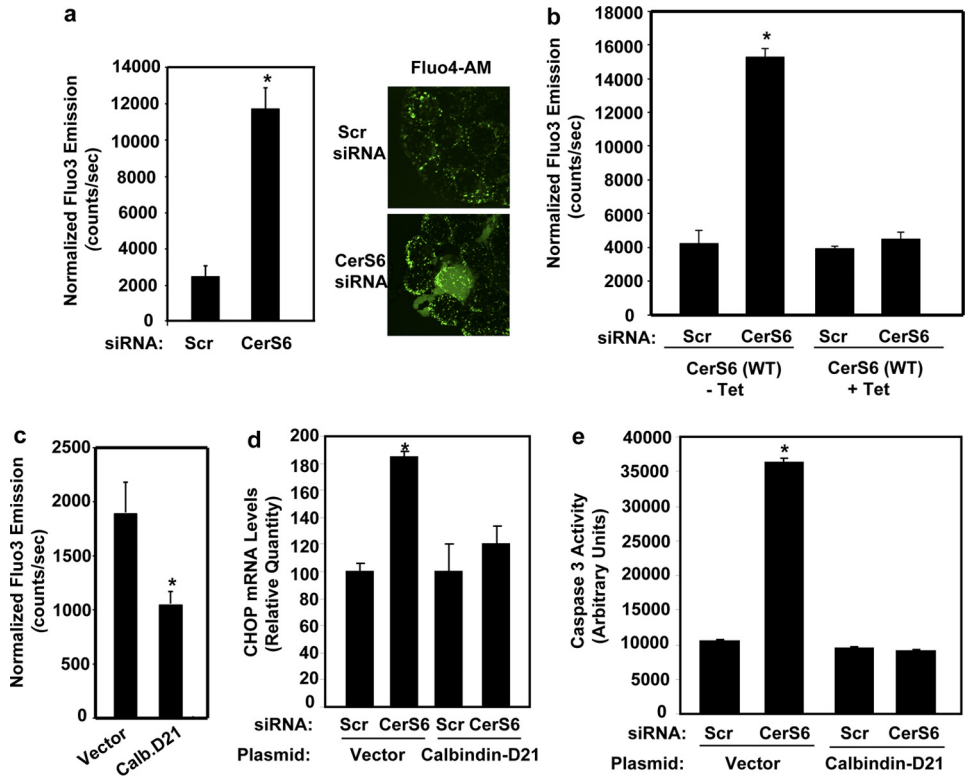

FIGURE 6. **Down-regulation of CerS6/C_{16}-ceramide activates ATF-6 via Ca^{2+} release from ER stores.** *a*, UM-SCC-22A cells were transfected with Scr or CerS6 siRNAs (50 nM, 48 h), and $[Ca^{2+}]_{In}$ levels were measured with Fluo3 as described under "Experimental Procedures" (*left panel*), or $[Ca^{2+}]_{In}$ was visualized with Fluo4 by confocal microscopy (*right panel*). *b*, cells stably expressing Tet-inducible WT CerS6 were uninduced (−*Tet*) or induced (+*Tet*) and transfected with either Scr or CerS6 siRNAs (50 nM, 48 h), and $[Ca^{2+}]_{In}$ levels were measured with Fluo3. *c*, UM-SCC-22A cells were transfected with vector or calbindin-expressing plasmids, and $[Ca^{2+}]_{In}$ levels were measured with Fluo3. *d* and *e*, UM-SCC-22A cells were transiently transfected with either control (*Vector*) or calbindin-expressing plasmids in the presence of Scr or CerS6 siRNA (50 nM, 48 h) transfection, and CHOP mRNA levels (*d*) and caspase 3 activity (*e*) were measured. In *a*–*d*, bar graphs show the mean ± S.E. from three independent experiments performed in duplicate. Student's *t* test was performed, and $p < 0.05$ (*) was considered significant.

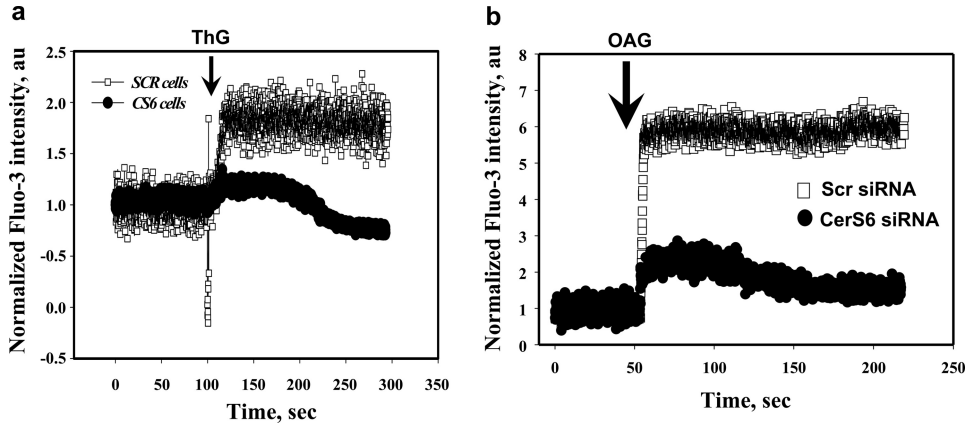

FIGURE 7. **Knockdown of CerS6/C_{16}-ceramide causes Ca^{2+} release from ER stores.** *a* and *b*, UM-SCC-22A cells were transfected with either Scr or CerS6 siRNA (50 nM, 48 h), and $[Ca^{2+}]_{In}$ levels in response to ThG (*a*) or 1-oleoyl-2-acyl-*syn*-glycerol (*OAG*; *b*) were measured as described under "Experimental Procedures." These data are representative of three independent trials. *au*, absorbance units.

facilitated the ER/Golgi association of ATF-6 for its cleavage and activation by S1P/S2P proteases. To examine this view, localization of ATF-6-FLAG, ectopically expressed using transient transfections, and the Golgi membranes in response to CerS6 knockdown was visualized by confocal microscopy using anti-FLAG (*red*) and anti-GM130 (*green*) antibodies compared with controls. Indeed, down-regulation of CerS6 resulted in Golgi fragmentation and increased the co-localization of ATF-6-FLAG with the fragmented Golgi/ER membrane network, and ectopic expression of calbindin prevented the Golgi fragmentation and ATF-6 activation (Fig. 9*f*). Thus, these data suggested that ATF-6 activation by knockdown of CerS6 requires a two-step process that is dependent on perturbation of $[Ca^{2+}]_{ER}$ via down-regulation of SERCA2/3, which then results in fragmentation of Golgi membranes that facilitated the ER/Golgi association of ATF-6 for its activation. Accordingly, down-regulation of SERCA2/3 using siRNAs in combination with increased Golgi fragmentation using brefeldin A induced ATF6

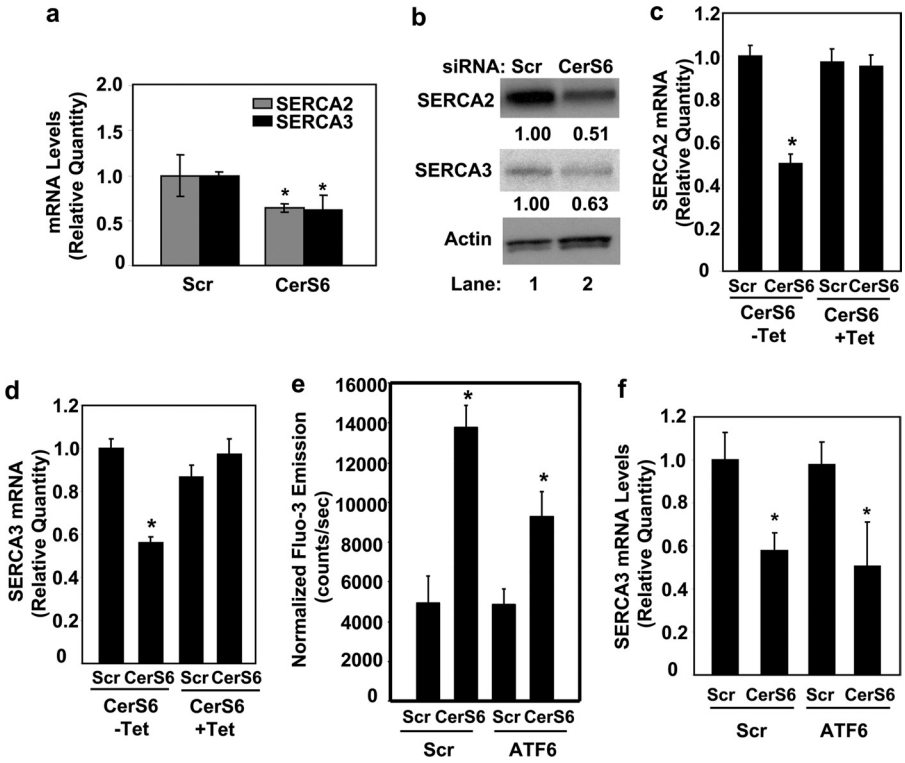

FIGURE 8. **Down-regulation of CerS6/C_{16}-ceramide causes calcium release from ER stores via SERCA2 and -3 down-regulation.** *a*, UM-SCC-22A cells were transfected with either Src or CerS6 siRNA (50 nM, 48 h), and calcium release from ER stores in response to ThG was measured as described under "Experimental Procedures." *b*, UM-SCC-22A cells were transfected with Scr or CerS6 siRNA, and their effect on SERCA2 and -3 mRNA (*left panel*) and protein (*right panel*) levels was detected by Q-PCR and Western blotting, respectively. *c* and *d*, cells stably expressing Tet-inducible wild type CerS6 were either uninduced (−*Tet*) or induced (+*Tet*) and transfected with Scr or CerS6 siRNAs (50 nM, 48 h), and their effects on SERCA2 (*c*) and SERCA3 (*d*) mRNA levels were measured by Q-PCR. *e* and *f*, UM-SCC-22A cells were double-transfected in combination with either Scr or ATF-6 siRNAs and Scr or CerS6 siRNAs (50 nM, 48 h), and $[Ca^{2+}]_{in}$ levels (*e*) and SERCA3 mRNA levels (*f*) were measured with Fluo3 labeling and Q-PCR, respectively. In *b*, blot pictures are representative of three independent experiments. Relative band intensities were measured with Image J software and are presented under the bands. *Bar graphs* show the mean ± S.E. from three independent experiments performed in duplicate. Student's *t* test was performed, and $p < 0.05$ (*) was considered significant.

activation about 2.5-fold compared with controls (Fig. 9*c*), measured by induction of CHOP mRNA expression and caspase-3 activation (Fig. 9*d*), supporting the two-step mechanism, involving perturbation of $[Ca^{2+}]_{ER}$ and the Golgi/ER membrane co-localization for the activation of ATF-6 in response to CerS6 knockdown.

Down-regulation of CerS6/C_{16}-ceramide Leads to the Fusion of the Golgi into the ER Membranes—Then, it was important to confirm that ATF-6 activation, in response to CerS6 knockdown and perturbation of $[Ca^{2+}]_{ER}$, is mediated by the fusion of the Golgi into the ER membranes, exposing pro-ATF-6 to site-1 and site-2 proteases. It is well established that BFA-induced fusion of the Golgi into the ER results in the modification of carbohydrate chains of ER resident proteins by Golgi glycosyltransferases (36–38), which can be evaluated *in vitro* by resistance to Endo H digestion. It is known that upon modification by Golgi glycosyltransferases, the ER resident proteins gain resistance to Endo H digestion due to modifications with complex oligosaccharides (36, 37). Therefore, to examine Golgi fragmentation and co-localization/fusion with ER membranes upon down-regulation of CerS6/C_{16}-ceramide, we examined the carbohydrate chain modification of the ER-targeted inhibitor 2 of protein phosphatase 2A (I2PP2A-ER-GFP) oncoprotein using Endo H cleavage. I2PP2A protein, which is nuclear, was targeted to the ER by removal of nuclear localization signals (NLS1 and NLS2) and the addition of the ER retention signal (KDEL) at its C terminus (Fig. 10*a*). Next, we confirmed cellular localization of wild type (I2PP2A-WT-GFP) and the I2PP2A-ER-GFP by immunofluorescence and confocal microscopy. Although I2PP2A-WT-GFP localized in the nucleus, I2PP2A-ER-GFP was co-localized with an ER resident calnexin (*red*), verifying cellular localization at the ER (*yellow*) (Fig. 10*b*).

Then we investigated carbohydrate modification of I2PP2A-ER-GFP *versus* endogenous I2PP2A, which is nuclear, in the absence/presence of BFA. In the absence of BFA, I2PP2A-ER-GFP was sensitive to Endo H cleavage, causing a slightly faster migration of the protein on SDS-PAGE compared with untreated controls (Fig. 10*c*, *lanes 2* and *1*, respectively). In BFA-treated cells, however, Endo H treatment had no detectable effect on I2PP2A-ER-GFP migration compared with controls (Fig. 10*c*, *lanes 4* and *3*, respectively) due to fusion of the disrupted Golgi with ER membranes, as reported previously (36–38). As expected, there was no shift in the molecular weight of endogenous I2PP2A in response to Endo H treatment in the presence of BFA (Fig. 10*c*, *lower panel*, *lanes 1–4*). Thus, these data confirmed that carbohydrate modification of I2PP2A-ER-GFP can be used for evaluation of functional distribution and fusion of the Golgi into the ER membranes.

Moreover, we examined the effects of siRNA-mediated CerS6 knockdown in this process. The data showed that I2PP2A-ER-GFP was sensitive to Endo H cleavage in UM-SCC-22A cells transfected with control (Scr) siRNAs compared with

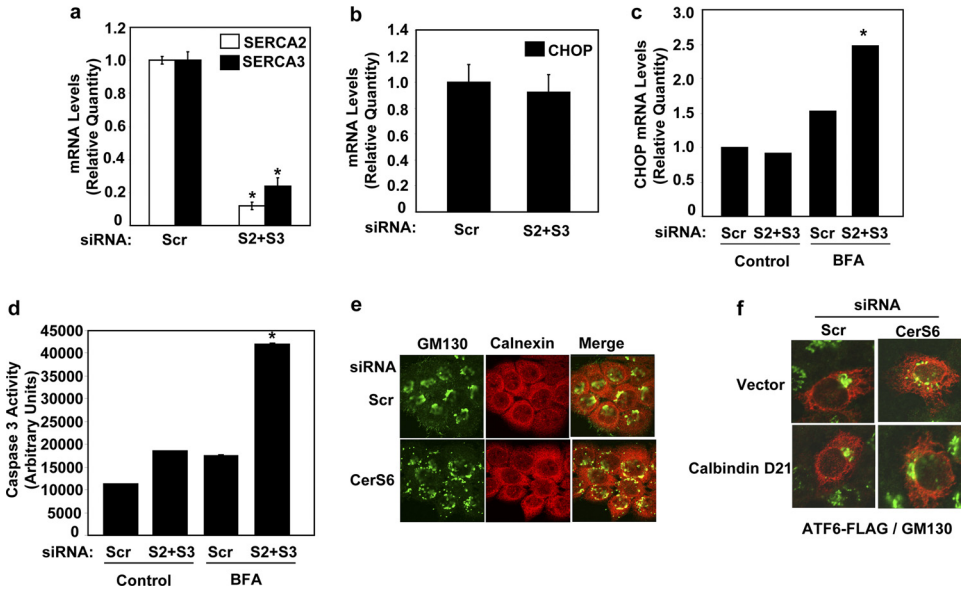

FIGURE 9. **CerS6/C_{16}-ceramide regulates ER/Golgi membrane network.** *a* and *b*, UM-SCC-22A cells were transfected with either Scr (100 nM) or SERCA2 and SERCA3 (50 nM each) in combination siRNAs for 48 h, and their effects on SERCA2 and -3 (*a*) and CHOP (*b*) mRNA levels were detected by Q-PCR. *c* and *d*, cells transfected with Scr or SERCA2 and SERCA3 siRNAs (48 h) in combination were treated with BFA (10 μg/ml, 3 h), and CHOP mRNA levels (*c*) and activation of caspase 3 (*d*) were measured by Q-PCR and a caspase 3 activity assay kit, respectively. *e*, cells transfected with Scr or CerS6 siRNA were fixed, and cellular localization of calnexin and GM130 were determined by immunofluorescence staining and confocal microscopy as described under "Experimental Procedures." *f*, cells were co-transfected with FLAG-tagged ATF-6 and either control (vector) or calbindin-expressing plasmids for 48 h. Next, Scr or CerS6 siRNA (50 nM) siRNA transfections were performed, and cellular localization of FLAG-tagged ATF6 and GM130 was visualized by immunofluorescence staining and confocal microscopy. *Graphs* show the mean ± S.E. from three independent experiments performed in duplicate. Student's *t* test was performed, and $p < 0.05$ (*) was considered significant. In *e* and *f*, micrographs are representative of at least three fields in two independent experiments.

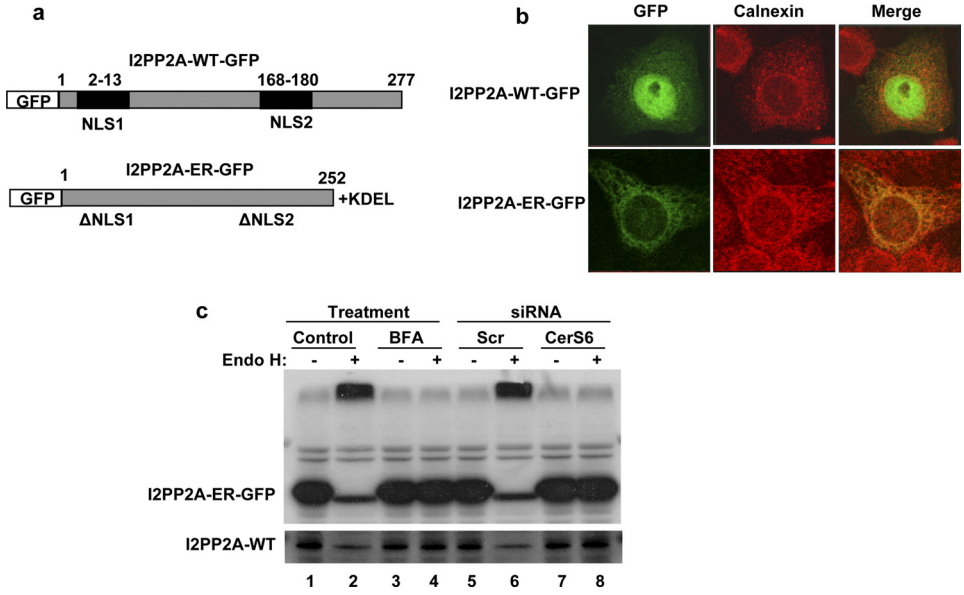

FIGURE 10. **Down-regulation of CerS6/C_{16}-ceramide leads to the fusion of disrupted Golgi into the ER membranes.** *a*, schematic representation of I2PP2A-WT-GFP and I2PP2A-ER-GFP proteins is shown. *b*, UM-SCC-22A cells were transfected with plasmids expressing I2PP2A-WT or I2PP2A-ER with GFP tags. Cellular localization of expressed proteins was determined by immunofluorescence staining of calnexin and confocal microscopy as described under "Experimental Procedures." *c*, UM-SCC-22A cells were transfected with the plasmid expressing I2PP2A-ER-GFP for 48 h and either treated with vehicle or BFA (10 μg/ml, for 3 h) or transfected with Scr or CerS6 siRNAs (50 nM, 48 h). Carbohydrate modification of endogenous I2PP2A and I2PP2A-ER-GFP by Golgi fusion was determined by Endo H treatment of lysates as described under "Experimental Procedures." In *b*, micrographs are representative of at least three fields in two independent experiments. In *c* data represent at least three independent experiments.

controls (Fig. 10*c*, *lanes 6* and *5*, respectively). In contrast, I2PP2A-ER-GFP exerted resistance to Endo H treatment in response to siRNA-mediated CerS6 knockdown compared with controls (Fig. 10*c*, *lanes 8* and *7*, respectively). It should be noted that Endo H treatment also resulted in the accumulation of very high molecular weight proteins due to undefined mechanisms, which were relieved by BFA treatment or CerS6 knockdown (Fig 10*c*, *lanes 2* and *4* or *lanes 6* and *8*, respectively). Thus, these data support that down-regulation of Cer6/C_{16}-ceramide disrupts the ER/Golgi membrane network and leads to the fusion of the Golgi with the ER membranes, where pro-ATF-6 is activated.

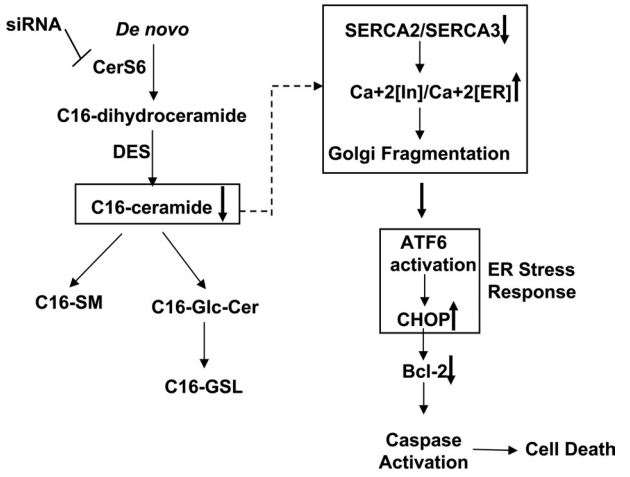

FIGURE 11. **Schematic representation of the mechanisms involved in activation of ATF-6 arm of ER stress response by down-regulation of CerS6/C_{16}-ceramide.** ATF-6 activation was regulated by a concerted two-step process involving the release of Ca^{2+} from the ER stores ($[Ca^{2+}]_{ER}$) via down-regulation of SERCA2/SERCA3, which resulted in the fragmentation of Golgi membranes in response to CerS6/C_{16}-ceramide alteration. This then leads to the accumulation of pro-ATF-6 in the disrupted ER/Golgi membrane network, where pro-ATF6 is cleaved and activated by S1P/S2P proteases, inducing CHOP-mediated apoptosis. *DES,* Desaturase; *GSL,* Glycosphingolipids.

DISCUSSION

Here we describe a novel mechanism involved in the selective activation of ATF-6 in response to CerS6/C_{16}-ceramide down-regulation via perturbation of $[Ca^{2+}]_{ER}/[Ca^{2+}]_{In}$, leading to disruption of ER/Golgi membrane network and subsequent CHOP-induced apoptosis (Fig. 11). This process appears to be operational in multiple head and neck and lung cancer cell lines with squamous carcinoma origin.

Consistent with out previous study (21), we show here that although induction of wt-, but not catalytically inactive mutant-CerS6, induces HNSCC tumor growth, knockdown of CerS6 mediates ATF-6 activation and apoptosis. Interestingly, treatment with tunicamycin and SAHA resulted in proteasome-dependent degradation of CerS6, leading to cell death. Stress-induced ubiquitination and proteasomal degradation of CerS1 were shown previously (39); however, regulation of CerS6 degradation by ER stress inducers has not been described previously.

Mechanistically, our data indicated that alteration of $[Ca^{2+}]_{ER}/[Ca^{2+}]_{In}$ rheostat plays a key role in the activation of ATF-6 in response to CerS6 knockdown. These data are in agreement with a previous report which showed that elevation of $[Ca^{2+}]_{In}$ is an upstream regulator for ATF-6 activation (28). These data also revealed the importance of the inhibition of SERCA expression in ATF-6 activation in response to Cer6/C_{16}-ceramide down-regulation. Although a role for exogenous ceramides in the regulation of apoptosis via alterations of cellular Ca^{2+} homeostasis has been described previously (40), data presented here are novel because roles of CerS-generated endogenous ceramides in the regulation of $[Ca^{2+}]_{ER}/[Ca^{2+}]_{In}$ rheostat by SERCA modulation have not been described previously. It was also revealed that gangliosides GM2, GM1, and GM3 inhibit Ca^{2+} uptake via SERCA in neurons and in brain microsomes, and an exposed carboxyl group on the ganglioside sialic acid residue is required for inhibition (41). Interestingly, these data demonstrated that the saccharides must be attached to a ceramide backbone to inhibit SERCA, as the ceramide-free ganglioside saccharide was not very efficient to inhibit SERCA (41).

In addition, fragmentation of Golgi membranes by alterations of $[Ca^{2+}]_{ER}/[Ca^{2+}]_{In}$ rheostat via inhibition of SERCA in response to CerS6/C_{16}-ceramide knockdown increased the co-localization of ATF-6 with ER/Golgi network, where it is cleaved by S1P/S2P proteases for activation (8). Interestingly, knockdown of CerS6 did not simply induce the translocation of pro-ATF-6 to Golgi for its activation, but it mediated the co-localization of Golgi membranes with the ER and pro-ATF-6, inducing ATF-6 activation. This was similar to the effects of siRNA mediated inhibition of GBF1 on ATF-6 activation in which treatment with GBF1 siRNA induced co-localization of ER/Golgi membranes for its cleavage/activation by S1P/S2P proteases without affecting the translocation of pro-ATF-6 to the Golgi (42). Importantly, our novel data also suggest that perturbation of the Golgi/ER membrane network, leading to the fusion of the Golgi with the ER membranes, is regulated by increased $[Ca^{2+}]_{In}/[Ca^{2+}]_{ER}$, and calbindin expression prevented Golgi fragmentation, ATF-6 activation, and apoptosis in response to CerS6 knockdown. In contrast, alterations of $[Ca^{2+}]_{In}/[Ca^{2+}]_{ER}$ by induction of CerS6/C_{16}-ceramide metabolism in response to vorinostat and sorafenib have been reported to play a role in the inhibition of gastrointestinal cancer growth (29). To this end, it will be interesting to determine whether subcellular localization of CerS6-generated C_{16}-ceramide in the ER/Golgi *versus* mitochondria (43, 44) membranes, where C_{16}-ceramide is apoptotic, plays a role in the regulation of apoptotic *versus* anti-apoptotic effects of CerS6-generated C_{16}-ceramide in different cell types. Notably, depletion of sphingosine-1-phosphate phosphohydrolase-1, an ER resident enzyme that specifically dephosphorylates S1P, induced pro-survival ER stress and autophagy concomitant with an increased intracellular pool of anti-apoptotic lipid S1P, but not dihydro-S1P (45), suggesting a diverse functions of sphingolipids in the regulation of ER stress and cell death.

The diverse functions of ceramides containing different fatty acid chain lengths were also supported by various recent studies (46, 47). For example, overexpression of C_{16}-ceramide generated by CerS5 but not by CerS6 was shown to significantly increase IR-induced apoptosis, and overexpression of CerS2 for the generation of $C_{24:0}$- and $C_{24:1}$-ceramides conferred protection against IR-induced apoptosis (48). Interestingly, *schlank* was identified as a CerS homologue in *Drosophila* (49) recently, and a mutation of *schlank* reduced *de novo* ceramide generation and drastically decreased larval growth. Interestingly, recent data (50) suggest that elevated C_{16}-ceramide associate with a positive lymph node status in breast cancer patients, indicating the metastatic potential of C_{16}-ceramide in the clinic. In another published report, elevated CerS2 and CerS6 mRNA was observed in breast cancer tumors (51). Thus, these data indicate that distinct functions of ceramides with different fatty acid chain lengths might not be limited to HNSCC or squamous lung cancers but can be observed in other cancer cell types also.

In summary, this study describes a novel mechanism for ATF-6 activation, and subsequent apoptosis is mediated via perturbation of $[Ca^{2+}]_{ER}$ and the ER/Golgi membrane network in response to knockdown of CerS6 and reduced C_{16}-ceramide generation in human head and neck and lung cancer cells with squamous carcinoma origin. Although the mechanisms of the cell/tissue-type selectivity of this process is still unknown, these data might have significant implications for the development of novel therapeutics against squamous cell carcinomas by targeted inhibition/degradation of CerS6. Therefore, identification of the molecular mechanisms of how ceramides exert their distinct functions based on fatty acid composition has important clinical relevance especially to generate mechanism-driven novel therapeutic strategies against some human cancers.

Acknowledgments—Human HNSCC cell lines UM-SCC-1, UM-SCC-14A, and UM-SCC-22A cells were kindly provided by Dr. Thomas Carey (University of Michigan). The dominant-negative-ATF6 cDNA was kindly provided by Dr. Christopher Glembotski (University of California, San Diego). Lung cancer cell lines were obtained from Dr. Harry Drabkin (Medical University of South Carolina). The core facilities utilized for animal studies and Lipidomics were constructed using support from the National Institutes of Health (Grant C06 RR015455) at the Extramural Research Facilities Program of the National Center for Research Resources.

REFERENCES

1. Szegezdi, E., Logue, S. E., Gorman, A. M., and Samali, A. (2006) *EMBO Rep.* **7,** 880–885
2. Ron, D., and Walter, P. (2007) *Nat. Rev. Mol. Cell Biol.* **8,** 519–529
3. Harding, H. P., Zhang, Y., Bertolotti, A., Zeng, H., and Ron, D. (2000) *Mol. Cell* **5,** 897–904
4. Wang, X. Z., Harding, H. P., Zhang, Y., Jolicoeur, E. M., Kuroda, M., and Ron, D. (1998) *EMBO J.* **17,** 5708–5717
5. Wang, Y., Shen, J., Arenzana, N., Tirasophon, W., Kaufman, R. J., and Prywes, R. (2000) *J. Biol. Chem.* **275,** 27013–27020
6. Marciniak, S. J., and Ron, D. (2006) *Physiol. Rev.* **86,** 1133–1149
7. Yoshida, H., Matsui, T., Yamamoto, A., Okada, T., and Mori, K. (2001) *Cell* **107,** 881–891
8. Shen, J., and Prywes, R. (2004) *J. Biol. Chem.* **279,** 43046–43051
9. Haze, K., Okada, T., Yoshida, H., Yanagi, H., Yura, T., Negishi, M., and Mori, K. (2001) *Biochem. J.* **355,** 19–28
10. Okada, T., Yoshida, H., Akazawa, R., Negishi, M., and Mori, K. (2002) *Biochem. J.* **366,** 585–594
11. Ma, Y., Brewer, J. W., Diehl, J. A., and Hendershot, L. M. (2002) *J. Mol. Biol.* **318,** 1351–1365
12. McCullough, K. D., Martindale, J. L., Klotz, L. O., Aw, T. Y., and Holbrook, N. J. (2001) *Mol. Cell. Biol.* **21,** 1249–1259
13. Zinszner, H., Kuroda, M., Wang, X., Batchvarova, N., Lightfoot, R. T., Remotti, H., Stevens, J. L., and Ron, D. (1998) *Genes Dev.* **12,** 982–995
14. Hanada, K., Kumagai, K., Yasuda, S., Miura, Y., Kawano, M., Fukasawa, M., and Nishijima, M. (2003) *Nature* **426,** 803–809
15. D'Angelo, G., Polishchuk, E., Di Tullio, G., Santoro, M., Di Campli, A., Godi, A., West, G., Bielawski, J., Chuang, C. C., van der Spoel, A. C., Platt, F. M., Hannun, Y. A., Polishchuk, R., Mattjus, P., and De Matteis, M. A. (2007) *Nature* **449,** 62–67
16. Mizutani, Y., Kihara, A., and Igarashi, Y. (2005) *Biochem. J.* **390,** 263–271
17. Pewzner-Jung, Y., Ben-Dor, S., and Futerman, A. H. (2006) *J. Biol. Chem.* **281,** 25001–25005
18. Michel, C., van Echten-Deckert, G., Rother, J., Sandhoff, K., Wang, E., and Merrill, A. H., Jr. (1997) *J. Biol. Chem.* **272,** 22432–22437
19. Lahiri, S., and Futerman, A. H. (2005) *J. Biol. Chem.* **280,** 33735–33738
20. Venkataraman, K., Riebeling, C., Bodennec, J., Riezman, H., Allegood, J. C., Sullards, M. C., Merrill, A. H., Jr., and Futerman, A. H. (2002) *J. Biol. Chem.* **277,** 35642–35649
21. Senkal, C. E., Ponnusamy, S., Bielawski, J., Hannun, Y. A., and Ogretmen, B. (2010) *FASEB J.* **24,** 296–308
22. Bielawski, J., Szulc, Z. M., Hannun, Y. A., and Bielawska, A. (2006) *Methods* **39,** 82–91
23. Senkal, C. E., Ponnusamy, S., Rossi, M. J., Sundararaj, K., Szulc, Z., Bielawski, J., Bielawska, A., Meyer, M., Cobanoglu, B., Koybasi, S., Sinha, D., Day, T. A., Obeid, L. M., Hannun, Y. A., and Ogretmen, B. (2006) *J. Pharmacol. Exp. Ther.* **317,** 1188–1199
24. Manevich, Y., Townsend, D. M., Hutchens, S., and Tew, K. D. (2010) *PLoS One* **5,** e14151
25. Senkal, C. E., Ponnusamy, S., Rossi, M. J., Bialewski, J., Sinha, D., Jiang, J. C., Jazwinski, S. M., Hannun, Y. A., and Ogretmen, B. (2007) *Mol. Cancer Ther.* **6,** 712–722
26. Mukhopadhyay, A., Saddoughi, S. A., Song, P., Sultan, I., Ponnusamy, S., Senkal, C. E., Snook, C. F., Arnold, H. K., Sears, R. C., Hannun, Y. A., and Ogretmen, B. (2009) *FASEB J.* **23,** 751–763
27. Karahatay, S., Thomas, K., Koybasi, S., Senkal, C. E., Elojeimy, S., Liu, X., Bielawski, J., Day, T. A., Gillespie, M. B., Sinha, D., Norris, J. S., Hannun, Y. A., and Ogretmen, B. (2007) *Cancer Lett.* **256,** 101–111
28. Thuerauf, D. J., Hoover, H., Meller, J., Hernandez, J., Su, L., Andrews, C., Dillmann, W. H., McDonough, P. M., and Glembotski, C.C. (2001) *J. Biol. Chem.* **276,** 48309–48317
29. Park, M. A., Mitchell, C., Zhang, G., Yacoub, A., Allegood, J., Häussinger, D., Reinehr, R., Larner, A., Spiegel, S., Fisher, P. B., Voelkel-Johnson, C., Ogretmen, B., Grant, S., and Dent, P. (2010) *Cancer Res.* **70,** 6313–6324
30. Tafesse, F. G., Huitema, K., Hermansson, M., van der Poel, S., van den Dikkenberg, J., Uphoff, A., Somerharju, P., and Holthuis, J. C. (2007) *J. Biol. Chem.* **282,** 17537–17547
31. Vacaru, A. M., Tafesse, F. G., Ternes, P., Kondylis, V., Hermansson, M., Brouwers, J. F., Somerharju, P., Rabouille, C., and Holthuis, J. C. (2009) *J. Cell Biol.* **185,** 1013–1027
32. Hisatsune, C., Nakamura, K., Kuroda, Y., Nakamura, T., and Mikoshiba, K. (2005) *J. Biol. Chem.* **280,** 11723–11730
33. Brini, M., and Carafoli, E. (2009) *Physiol. Rev.* **89,** 1341–1378
34. Balla, T. (2009) *Cell Calcium* **45,** 527–534
35. Wojcikiewicz, R. J., Pearce, M. M., Sliter, D. A., and Wang, Y. (2009) *Cell Calcium* **46,** 147–153
36. Lippincott-Schwartz, J., Yuan, L. C., Bonifacino, J. S., and Klausner, R. D. (1989) *Cell* **56,** 801–813
37. Lippincott-Schwartz, J., Glickman, J., Donaldson, J. G., Robbins, J., Kreis, T. E., Seamon, K. B., Sheetz, M. P., and Klausner, R. D. (1991) *J. Cell Biol.* **112,** 567–577
38. Doms, R. W., Russ, G., and Yewdell, J. W. (1989) *J. Cell Biol.* **109,** 61–72
39. Sridevi, P., Alexander, H., Laviad, E. L., Min, J., Mesika, A., Hannink, M., Futerman, A. H., and Alexander, S. (2010) *Exp. Cell Res.* **316,** 78–91
40. Scorrano, L., Oakes, S. A., Opferman, J. T., Cheng, E. H., Sorcinelli, M. D., Pozzan, T., and Korsmeyer, S. J. (2003) *Science* **300,** 135–139
41. Ginzburg, L., Li, S. C., Li, Y. T., and Futerman, A. H. (2008) *J. Neurochem.* **104,** 140–146
42. Citterio, C., Vichi, A., Pacheco-Rodriguez, G., Aponte, A. M., Moss, J., and Vaughan, M. (2008) *Proc. Natl. Acad. Sci. U.S.A.* **105,** 2877–2882
43. Lee, H., Rotolo, J. A., Mesicek, J., Penate-Medina, T., Rimner, A., Liao, W. C., Yin, X., Ragupathi, G., Ehleiter, D., Gulbins, E., Zhai, D., Reed, J. C., Haimovitz-Friedman, A., Fuks, Z., and Kolesnick, R. (2011) *PLoS One* **6,** e19783
44. Ogretmen, B., and Hannun, Y. A. (2004) *Nat. Rev. Cancer* **4,** 604–616
45. Lépine, S., Allegood, J. C., Park, M., Dent, P., Milstien, S., and Spiegel, S. (2011) *Cell Death Differ* **18,** 350–361
46. Hannun, Y. A., and Obeid, L. M. (2011) *J. Biol. Chem.* **286,** 27855–27862
47. Ponnusamy, S., Meyers-Needham, M., Senkal, C. E., Saddoughi, S. A., Sentelle, D., Selvam, S. P., Salas, A., and Ogretmen, B. (2010) *Future Oncol.*

6, 1603–1624
48. Mesicek, J., Lee, H., Feldman, T., Jiang, X., Skobeleva, A., Berdyshev, E. V., Haimovitz-Friedman, A., Fuks, Z., and Kolesnick, R. (2010) *Cell. Signal.* **22,** 1300–1307
49. Bauer, R., Voelzmann, A., Breiden, B., Schepers, U., Farwanah, H., Hahn, I., Eckardt, F., Sandhoff, K., and Hoch, M. (2009) *EMBO J.* **28,** 3706–3716
50. Schiffmann, S., Sandner, J., Birod, K., Wobst, I., Angioni, C., Ruckhäberle, E., Kaufmann, M., Ackermann, H., Lötsch, J., Schmidt, H., Geisslinger, G., and Grösch, S. (2009) *Carcinogenesis* **30,** 745–752
51. Erez-Roman, R., Pienik, R., and Futerman, A. H. (2010) *Biochem. Biophys. Res. Commun.* **391,** 219–223